超声波振动在 Ce-Zr-La/Al₂O₃ 及负载型 Pd 三效催化剂制备中的应用

蔡 黎　　王康才　　赵 明　　龚茂初　　陈耀强 *

(四川大学化学学院, 绿色化学教育部重点实验室, 成都　610064)

摘要：　制备了 CeO₂-ZrO₂-La₂O₃/Al₂O₃ 材料, 在制备过程中使用超声波振动对材料进行处理, 并以此材料为载体制备了单 Pd 三效催化剂. 对所制备的载体进行了织构性能分析(BET)和 X 射线衍射(XRD)表征. 对催化剂进行了 NO 程序升温脱附(NO-TPD)及 H₂ 程序升温还原(H₂-TPR)表征, 并对催化剂进行了活性测试. BET 结果表明, 900 ℃焙烧后, 超声波振动处理的载体比表面积为 130 m²·g⁻¹, 而没有进行处理的载体比表面积为 117 m²·g⁻¹. 超声波处理的 CeO₂-ZrO₂-La₂O₃/Al₂O₃ 材料介孔直径为 11.4 nm, 相对较大, 载体更加稳定. XRD 测试结果表明, 超声波处理的载体在 1150 ℃焙烧 5 h 后仍然只有 Ce₀.₅Zr₀.₅O₂ 一个单一物相, 而未经过超声波处理的载体此时出现相分离, 体相中有 *θ*-Al₂O₃ 出现. 以超声波处理材料为载体的 Pd 催化剂新鲜和老化后 NO-TPD 测试结果变化很小. H₂-TPR 测试中, 超声波振动处理的材料制备的催化剂中活性组分和载体的还原峰温较未超声处理材料制备的催化剂稍高, 而峰面积远大于未超声处理材料制备的催化剂. 活性测试结果说明, 由超声波振动处理过的载体制备的三效催化剂对汽车尾气中的三种污染物的起燃温度更低, 有更好的活性以及温度特性.

关键词：　Pd 三效催化剂;　催化活性;　NO 程序升温脱附;　H₂ 程序升温还原;　织构性能
中图分类号：　O643

Application of Ultrasonic Vibrations in the Preparation of Ce-Zr-La/Al₂O₃ and Supported Pd Three-Way-Catalyst

CAI Li　　WANG Kang-Cai　　ZHAO Ming　　GONG Mao-Chu　　CHEN Yao-Qiang*

(*Key Laboratory of Green Chemistry & Technology of the Ministry of Education, College of Chemistry, Sichuan University, Chengdu　610064, P. R. China*)

Abstract：　CeO₂-ZrO₂-La₂O₃/Al₂O₃ (CZLA) was prepared by pretreatment with ultrasonic vibrations and Pd three-way-catalysts (TWCs) were then synthesized. Supports were characterized using Brunauer-Emmett-Teller(BET) and X-ray diffraction (XRD). Pd catalysts were characterized using NO-temperature programmed desorption (NO-TPD), H₂-temperature programmed reduction (H₂-TPR) and a catalytic activity test. The specific surface area of the uv-CZLA (CZLA with ultrasonic vibration) and the n-CZLA (CZLA without ultrasonic vibration) was 130 and 117 m²·g⁻¹, respectively, after calcination at 900 ℃. The uv-CZLA material had larger pores of 11.4 nm and this made it more thermally stable than the n-CZLA. uv-CZLA supports were calcined at various temperatures and showed only one Ce₀.₅Zr₀.₅O₂ phase. However, *θ*-Al₂O₃ was observed in n-CZLA after aging at 1150 ℃ for 5 h. Almost no difference in NO-TPD was found for fresh and aged Pd/uv-CZLA catalysts. Results from the H₂-TPR of the Pd/uv-CZLA catalyst showed a higher reductive peak temperature and a far larger reducing peak area than that of Pd/n-CZLA. Results of three-way reactions show that the catalyst prepared using ultrasonic vibration treatment possesses a lower light-off temperature for the removal of all three main pollutants in vehicle emissions and also a better temperature property.

Key Words：　Pd three-way-catalyst;　Catalytic activity;　NO-TPD;　H₂-TPR;　Textural property

Pd three-way-catalyst (TWC) loaded on the support of CeO_2-ZrO_2 (CZ) solid solution[1-4] is well investigated. CeO_2-ZrO_2 is also called oxygen storage material (OSM) and has oxygen storage capacity (OSC) which can stabilize the redox environment by absorbing oxygen in an oxidative atmosphere and releasing oxygen in a reductive environment[5-9]. However, CZ solid solution is sintered easily under harsh condition and is less stable than some regular supports like alumina[10]. The dispersion and efficiency of active components are dependent on high specific surface area. More attentions have been drawn on co-impregnating CZ on alumina. In this way, the new material has both stable high surface area and OSC[11-13]. Many researches reported that co-impregnating was not the best way to prepare CZ/Al_2O_3. Our team had done some investigations on this subject by co-precipitation method[14,15]. The results show that co-precipitation is an efficient way to prepare CeO_2-ZrO_2/Al_2O_3 (CZA). CZA prepared by co-precipitation possesses both excellent textural property and thermal stability. With high Al_2O_3 content, mesopore material is stable after calcination at 900 ℃, and could work in harsh condition. Otherwise, mesopore materials prepared by using ultrasonic vibration method show narrow particle size distribution and similar sized interparticle mesopores[16]. Obviously, the ultrasonic treatment leads to a disintegration of the loosely attached aggregates, which guarantees the material with a narrower particle size distribution and higher specific surface area. Using ultrasonic vibration is an efficient way to modify the support of TWC. Meanwhile, Pt, Pd and Rh are widely used as the active component of TWCs. Pd is considered as the most useful one according to its price. In this paper, CeO_2-ZrO_2-La_2O_3/Al_2O_3 (CZLA) materials were prepared and characterized after various temperature calcination. Also, Pd/CZLA catalysts were prepared and investigated for the effects of ultrasonic vibration treatment on the preparation of CZLA and Pd-supported TWC.

1 Experimental

1.1 Preparation of supports

The supports were prepared by the co-precipitation method from the corresponding chemicals: $Ce(NO_3)_3 \cdot 6H_2O(AR)$, $ZrO(NO_3)_2$ (AR), $La(NO_3)_3(AR)$, and $Al(NO_3)_3(AR)$ in stoichiometric ratios. The precursors were separately mixed in an aqueous solution and then were added in drops to ultrasonic vibration instrument containing a mixed aqueous solution of ammonia and salvolatile. The precipitates were filtered, washed, and dried at 105 ℃ overnight, then calcined at 600 ℃ for 5 h. Finally, CZLA (CeO_2: 20%; ZrO_2: 20%; La_2O_3: 3%; Al_2O_3: 57% (*w*, mass fraction)) was obtained. Moreover, uv-CZLA was obtained with ultrasonic vibration treatment whereas n-CZLA was obtained in the same way but without ultrasonic vibration treatment. The supports were calcined at 900, 1000, 1050, 1100, 1150, and 1200 ℃ for 5 h, and marked as CZLA900, CZLA1000, CZLA1050, CZLA1100, CZLA1150, and CZLA1200, respectively.

1.2 Preparation of catalysts

The Pd/n-CZLA catalyst was prepared by impregnating n-CZLA900 with H_2PdCl_6 aqueous solution, then the catalyst was dried at 105 ℃ overnight and calcined at 500 ℃ for 3 h in air. After that, 4%(*w*) $La(NO_3)_3$ (AR), 3%(*w*) $ZrO(Ac)_2$ (AR), 2%(*w*) Ni-Al_2O_3(pre-prepared) as promoter and desired water were added, then ground to form a slurry. The resulting slurry was coated on a honeycomb cordierite (2.5 cm^3, Corning, America), then the washcoat was dried and calcined at 500 ℃ for 3 h in air. The Pd/uv-CZLA catalyst was prepared with uv-CZLA900 support as the same process mentioned above. In all the samples, the precious metal loading was 2 g·L^{-1}. Aged Pd/n-CZLA and aged Pd/uv-CZLA were obtained by calcined Pd/n-CZLA and Pd/uv-CZLA at 1000 ℃ for 5 h, respectively.

1.3 Characterization of supports and catalysts

The three-way catalytic reaction was investigated in a micro-reactor with the gas hourly space velocity (GHSV) of 3×10^4 h^{-1}. Reactant feed gas was a mixture of CO (0.86%), C_3H_8 (0.06%), NO (0.06%), CO_2 (10%), and vapor (10%) (φ, volume fraction), O_2 (adjustable), balanced by N_2. At a certain temperature, the concentrations of CO, C_3H_8, and NO were analyzed on-line by a five-component analyzer FGA24100 before and after the stimulated gas passing the micro-reactor.

The specific surface areas of the supports were measured by Brunauer-Emmet-Teller (BET) method at −196 ℃ using Autosorb-ZXF-05 (Xibei Chemistry Institute, China).

NO-TPD experiments were preformed in a quartz tubular micro-reactor. The sample (100 mg) was pretreated in a flow of argon (20 mL·min^{-1}) at 500 ℃ for 40 min, followed by cooling to room temperature (RT). Before a NO-TPD experiment was performed, the sample was pretreated to absorb NO (2%, balanced by N_2, 20 mL·min^{-1}) at RT for 45 min. Then the sample was heated from RT to 900 ℃ at a heating rate of 10 ℃·min^{-1} for NO desorption. The amount of desorbed NO was measured by a thermal conductivity detector (TCD).

Powder X-ray diffraction (XRD) was performed with a D/Max-rA Rotating Anode Diffractometer (Rigaku International Corp., Japan), Cu K_α radiation (λ=0.15418 nm) using graphite curved-crystal monochromator, operated at 40 kV and 100 mA with proportional counter detection for 2θ from 10° to 90°. The crystalline phases were identified by comparison with the reference data (PDF) from the International Center for Diffraction Data (ICDD)

H_2-TPR experiments were preformed in a quartz tubular micro-reactor. The sample (50 mg, 20−40 mesh) was pretreated in a flow of N_2 (40 mL·min^{-1}) at temperatures ranging from RT to 400 ℃ and maintained at 400 ℃ for 30 min. The reduction was performed with a 5% H_2-95% N_2 (30 mL·min^{-1}) mixture at a heating rate of 10 ℃·min^{-1} from RT to 900 ℃. The residual H_2 was detected by TCD.

2 Results and discussion

For all catalysts, the textural properties of supports have great influence on their activities. The textural properties of the supports after calcined at various temperatures are listed in Table

Table 1   Textural properties of the supports calcined at different temperatures for 5 h

$T/°C$	$S_{BET}/(m^2 \cdot g^{-1})$		$V_{pore}/(mL \cdot g^{-1})$		D_{pore}/nm	
	n-CZLA	uv-CZLA	n-CZLA	uv-CZLA	n-CZLA	uv-CZLA
600	140	187	0.40	0.52	10.7	11.3
900	117	130	0.35	0.42	10.9	11.4
1000	102	112	0.30	0.35	9.2	12.0
1050	89	103	0.24	0.32	8.3	10.6
1100	88	106	0.21	0.27	14.9	10.5
1150	40	78	0.14	0.18	21.8	13.2
1200	30	26	0.10	0.09	22.4	21.4

1. It is clear that both the specific surface area and the pore volume of uv-CZLA are bigger than those of n-CZLA after calcination at 600 – 1150 ℃. After calcination at 600 ℃, uv-CZLA possesses specific surface area of 187 m²·g⁻¹ and pore volume of 0.52 mL·g⁻¹, and these two main data remain 130 m²·g⁻¹ and 0.42 mL·g⁻¹ after calcination at 900 ℃. uv-CZLA is highly stable, even after calnation at 1150 ℃ for 5 h, the specific surface area is 78 m²·g⁻¹ and pore volume is 0.18 mL·g⁻¹. In the case of n-CZLA, after calcination at 600 ℃, the specific surface area and pore volume of n-CZLA are 140 m²·g⁻¹ and 0.40 mL·g⁻¹, respectively. After calcination at 900 ℃, they decrease to 117 m²·g⁻¹ and 0.35 mL·g⁻¹. So uv-CZLA is highly stable after calcination at 1150 ℃. n-CZLA shows less stability since the two main data sharply decrease to 40 m²·g⁻¹ and 0.14 mL·g⁻¹. Pd/n-CZLA catalyst would easily deactivate due to the encapsulation of active phase caused by the sharply decrease of specific surface area and pore volume. Accordingly, it is clear that ultrasonic vibration treatment improves the support textural property and stability. Furthermore, the ultrasonic vibration treatment also has great influence on the stability of the mesopores. It is easily understood that stable mesopore is related to better thermal stability. According to the research of Llusar and co-workers[17], bigger pore is related to better thermalstability. The average pore size of n-CZLA900 is 10.9 nm, smaller than 11.4 nm of uv-CZLA900. The pore diameter of n-CZLA1150 increases to 21.8 nm. The sharply increase of pore diameter

from 10.9 nm to 21.8 nm indicates the sinter of small mesopore and is related to the decrease of specific surface area. As mentioned above, uv-CZLA shows better performances in all these three aspects. It is reasonable that Pd/uv-CZLA catalyst has better catalytic activity and stability.

The nitrogen adsorption-desorption isotherms of the samples are clearly illustrated in Fig.1A. The nitrogen adsorption-desorption isotherms of the two given materials are type IV with great adsorption at high relative pressure, indicating the presence of mesopores. In the cases of both n-CZLA900 and uv-CZLA900, the isotherm curves present hysteresis loops, which manifest the standard H1 form[18,19], indicating the presence of cylindrical shaped mesopores. The hysteresis loop presented in the isotherm curves of uv-CZLA1150 changes into H2 form[20], which can be observed in the pores with narrow necks and wider bodies (ink bottle pores). For n-CZLA1150, it is still cylindrical shaped mesopores. The pore size distributions of the mesopores of the samples were analyzed and shown in Fig.1B. After calcination at 1150 ℃ for 5 h, mesopores around 5 nm of uv-CZLA disappear; this leads to a decrease in pore volume. On the other hand, 10 nm pore of n-CZLA congregates into larger pore about 20 nm, after calcined at 1150 ℃ for 5 h. It is plausible that the instability of n-CZLA pore causes the instability of the catalyst, and the change of activity of the catalyst will be discussed later.

Fig.2 shows the XRD patterns of the two materials calcined at 600, 900, and 1150 ℃. It is clear that the uv-CZLA samples show only the presence of $Ce_{0.5}Zr_{0.5}O_2$. The peaks of Al_2O_3 was not detected. It is plausible that two reasons for the absence of Al_2O_3. On one hand, Al^{3+} cations come into the $Ce_{0.5}Zr_{0.5}O_2$ cell, partially. However, with such high content of Al_2O_3 in this system, it is unreasonable for all Al^{3+} cations to get into the $Ce_{0.5}Zr_{0.5}O_2$ cells. On the other hand, there would be another part of Al_2O_3 remained amorphous. However, the underlying reason remains to be unraveled. After calcination at 1150 ℃ for 5 h, only single phase was observed, so uv-CZLA exhibits better thermal stability, which can be further proved by the BET results. At the same time, diffraction peaks of the uv-CZLA calcined at various tempera-
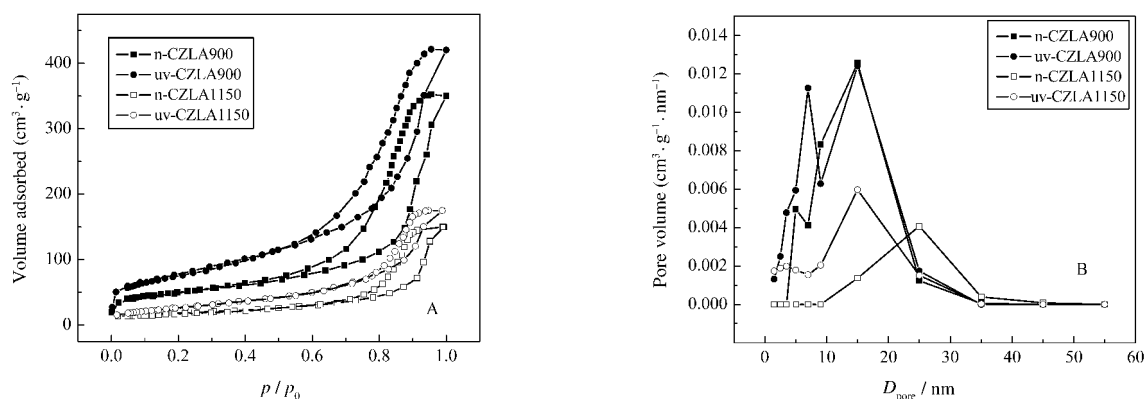
Fig.1   N₂ adsorption-desorption isotherms (A) and pore size distribution curves (B) of the two materials after calcined at 900 and 1150 ℃

n-CZLA900, n-CZLA1150: no ultrasonic vibration treated CeO₂-ZrO₂-LaO₂/Al₂O₃ calcined at 900 and 1150 ℃ for 5 h, respectively;

uv-CZLA900, uv-CZLA1150: ultrasonic vibration treated CeO₂-ZrO₂-LaO₂/Al₂O₃ calcined at 900 and 1150 ℃ for 5 h, respectively
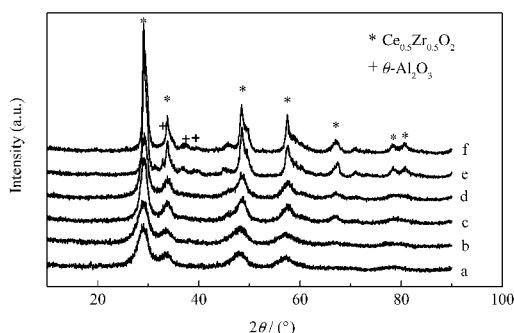
Fig.2   XRD patterns of supports after calcination at 600, 900, and 1150 ℃ for 5 h

a) n-CZLA600, b) uv-CZLA600, c) n-CZLA900, d) uv-CZLA900, e) n-CZLA1150, f) uv-CZLA1150

tures are broad and dispersive, which indicates that uv-CZLA exhibits a smaller crystallite size and excellent thermal stability. Therefore, it can be concluded that the good structure stability contributes greatly to the textural stability of uv-CZLA. The patterns of n-CZLA show no presence of Al_2O_3 phase but only $Ce_{0.5}Zr_{0.5}O_2$ phase after calcined at both 600 and 900 ℃ for 5 h. But after calcined at 1150 ℃ for 5 h, the XRD pattern of n-CZLA shows the presence of θ-Al_2O_3, which is the main reason for the instability.

The heterogeneous catalytic reaction is based on the adsorption and activation of reactants that concentrated on the surface of catalysts[21]. TWC, one of the most complex heterogeneous catalysts, works in the complicated environment, on which the adsorption of NO is one of the most important steps to remove the pollutants[21,22]. The NO-TPD measurements were performed for all the fresh and aged catalysts. As shown in Fig.3, there are four peaks on the NO-TPD pattern of Pd/n-CZLA. The research of Dimonte and co-workers[23] indicated that the peaks around 200 ℃ could be attributed to the desorption of NO adsorbed on the Pd monolayer surface. In their report, the peak at 350 ℃ is related to desorption of NO on the supports. Due to the strong interaction between NO and the support, the temperature of the NO desorption on the support is higher than that of the NO desorption on the Pd monolayer. Otherwise, Prinatto *et al.*[24] reported that the NO adsorption on the surface of the catalyst turned into the bulk
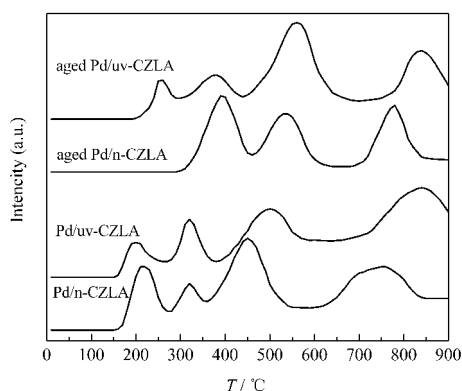
phase and formed nitrites and nitrates, and their decomposition took place at higher temperature of about 500 ℃(nitrite) and 800 ℃(nitrate), respectively. In this study, there are also four peaks over the NO-TPD curve of Pd/uv-CZLA. And the four peaks were produced in the same way to that of Pd/n-CZLA. Compared with the two NO-TPD curves of both Pd/n-CZLA and Pd/uv-CZLA, the peaks of nitrites and nitrate decomposition in Pd/uv-CZLA are higher than those of Pd/n-CZLA. Obviously, nitrite and nitrate in the bulk phase of Pd/uv-CZLA are more stable, so it shows that NO is more strongly absorbed and more active on Pd/uv-CZLA. In that case, Pd/uv-CZLA would perform better activity. As mentioned above, the sharp decrease of specific surface area and pore volume lead to the encapsulation of active phase Pd. The encapsulation of active phase would block the adsorption of NO to the Pd monolayer. So, the first peak in the NO-TPD curves over aged Pd/n-CZLA vanishes. The weakened adsorption of NO on the Pd monolayer causes the deactivation of NO and minimizes the activity of the catalyst. For the catalytic activity, aged Pd/n-CZLA does show worse catalytic performance than aged Pd/uv-CZLA. There are much greater difference between Pd/n-CZLA and aged Pd/n-CZLA than that between Pd/uv-CZLA and aged Pd/uv-CZLA, which also shows the instability of the non-treated material and better thermal stability of catalyst prepared by the ultrasonic vibration-treated supports.

The results of H_2-TPR test are showed in Fig.4. The negative peaks at about 100 ℃ in the H_2-TPR curves of all the fresh and aged catalysts are due to the desorption of H_2 adsorbed on the catalysts at RT. There are three other obvious peaks in all the four patterns. They could be attributed to the reduction of the active component, surface Ce^{4+}, and bulk Ce^{4+}, respectively. The peak temperature and the peak area are two basic parameters in the analysis of H_2-TPR tests. Lower the peak temperature is, easier the reduction happens, and the larger peak area is related to bigger amount of reductive species[12,14]. As shown in Fig.4, the reduction peak of the active component over Pd/n-CZLA and aged Pd/n-CZLA shows lower peak temperatures and smaller peak areas than those over Pd/uv-CZLA and aged Pd/uv-CZLA, respectively. In that case, reductive species in the Pd/uv-CZLA
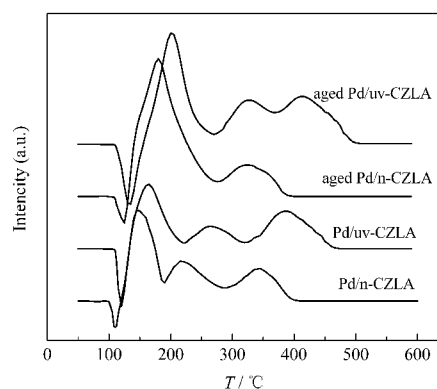

Fig.3   NO-TPD curves of the aged Pd/n-CZLA, aged Pd/ uv-CZLA, Pd/n-CZLA, and Pd/uv-CZLA catalysts

Fig.4   H₂-TPR profiles of the aged Pd/n-CZLA, aged Pd/ uv-CZLA, Pd/n-CZLA, and Pd/uv-CZLA catalysts

Table 2   Light-off properties of the catalysts at stoichiometric point

Sample	$T_{50\%}$/℃			$T_{90\%}$/℃			$(T_{90\%}-T_{50\%})$/℃		
	C$_3$H$_8$	CO	NO	C$_3$H$_8$	CO	NO	C$_3$H$_8$	CO	NO
Pd/n-CZLA	287	186	187	320	211	215	33	25	28
aged Pd/n-CZLA	350	277	289	392	333	342	42	56	53
Pd/uv-CZLA	274	173	188	300	196	210	26	23	22
aged Pd/uv-CZLA	327	240	247	364	287	300	37	47	53

catalysts are less active and are much more capable on the oxygen storage/release ability. Accordingly, Pd/uv-CZLA catalysts would be more active than Pd/n-CZLA. And the reaction discussed later would prove this point. There are two reduction peaks of Ce^{4+} in the H$_2$-TPR patterns. The lower CeO$_2$ content is, the better dispersion and easier reduction of Ce^{4+} will be. Accordingly, both the surface and bulk Ce^{4+} reduction peaks in this work are lower than that over CeO$_2$-ZrO$_2$[14]. After being aged, the reduction peak temperature of surface and bulk Ce^{4+} in the two catalysts rise because of the sinter of the support.

The catalytic performance is the most concern property to TWCs. Table 2 summaries the light-off temperatures ($T_{50\%}$) of the catalysts. Obviously, the Pd/uv-CZLA catalyst exhibits better catalytic activity. The light-off temperature of C$_3$H$_8$ over Pd/uv-CZLA is 274 ℃, which is about 10 ℃ lower than $T_{50\%}$ over Pd/n-CZLA. And the complete conversion temperature ($T_{90\%}$) of C$_3$H$_8$ on Pd/uv-CZLA is about 20 ℃ lower than that on Pd/n-CZLA. All the lower light-off temperatures indicate that Pd/uv-CZLA is more effective on the oxidation of hydrocarbon. $T_{50\%}$ and $T_{90\%}$ of NO and CO over Pd/uv-CZLA are also lower than those over Pd/n-CZLA. These two pollutants are also easier removed over Pd/uv-CZLA. After aged, both of the two catalysts show a deactivation behavior with the increase in $T_{50\%}$ and $T_{90\%}$. The $T_{50\%}$ and $T_{90\%}$ of C$_3$H$_8$ on aged Pd/uv-CZLA are 327 and 364 ℃, which are about 20 and 30 ℃ lower than those of aged Pd/n-CZLA, respectively. The elimination of C$_3$H$_8$ is more difficult than other reactants in the exhausted gas. Therefore, the conversion of C$_3$H$_8$ is one of the key points to assess the activity of TWCs[22]. As described in Table 2, the ΔT ($T_{90\%}-T_{50\%}$) values of C$_3$H$_8$ over both Pd/uv-CZLA and aged Pd/uv-CZLA are lower than that over Pd/n-CZLA and aged Pd/n-CZLA, respectively. It is also clear that the differences of the $T_{90\%}$ and $T_{50\%}$ of the reactants between Pd/uv-CZLA and aged Pd/uv-CZLA are slighter than that between Pd/n-CZLA and aged Pd/n-CZLA. And the slighter difference denotes better anti-aging property. From that mentioned above, it is clear that the Pd/uv-CZLA catalyst is more stable after high temperature thermal aging.

3   Conclusions

All the results indicate that the ultrasonic vibration can improve the textural properties of the CZLA supports. Material prepared with ultrasonic vibration pretreatment has higher specific surface area and larger pore volume. With bigger pore diameter, it shows excellent thermal stability. Ultrasonic vibration-pretreated material exhibits a more stable structure and remains one single Ce$_{0.5}$Zr$_{0.5}$O$_2$ phase after 1150 ℃ aging. The Pd/uv-

CZLA TWC has good thermal stability due to the great stability of uv-CZLA. On the other hand, because of the proper adsorption property of NO and larger amount of reductive species over the catalyst, the Pd/uv-CZLA catalyst shows lower light-off temperature and temperature property. All these show the advantage of using ultrasonic vibration in the preparation of CZLA.

References

1   Trovarelli, A. *Catal. Rev. -Sci. Eng.*, **1996, 38**: 439

2   Gandhi, H. S.; Graham, G. W.; McCabe, R. W. *J. Catal.*, **2003, 216**: 433

3   Kulyova, S. P.; Lunina, E. V.; Lunin, V. V.; Kostyuk, B. G.; Muravyova, G. P.; Kharlanov, A. N. *Chem. Mater.*, **2001, 13**: 1491

4   Ikryannikova, L. N.; Aksenov, A. A.; Markaryan, G. L.; Muraveva, G. P.; Kostyuk, B. G.; Kharlanov, A. N.; Lunina, E. V. *Appl. Catal. A*, **2001, 210**: 225

5   Eguchi, K.; Akasaka, N.; Mitsuyasu, H.; Nonaka, Y. *Solid State Ionics*, **2000, 135**: 589

6   Quinelato, A. L.; Longo, E.; Leite, E. R.; Bernardi, M. I. B.; Varela, J. A. *J. Mater. Sci.*, **2001, 36**: 3825

7   Djurado, E.; Meunier, E. *J. Solid State Chem.*, **1998, 141**: 191

8   Thammachart, M.; Meeyoo, V.; Risksomboon, T.; Osuwan, S. *Catal. Today*, **2001, 68**: 53

9   Hirano, M.; Miwa, T.; Inagaki, M. *J. Ceram. Soc. Jpn.*, **2001, 109**: 401

10   Terribile, D.; Trovarelli, A.; Llorca, J.; de Leitenburg, C.; Dolcetti, G. *J. Catal.*, **1998, 178**: 299

11   Dimonte, R.; Fornasiero, P.; Kaspar, J.; Graziani, M.; Gatica, J. M.; Bernal, S.; Gómez-Herrero, A. *Chem. Commun.*, **2000**: 2167

12   Iglesias-Juez, A.; Martínez-Arias, A.; Fernández-García, M. *J. Catal.*, **2004, 221**: 148

13   Yao, M. H.; Baird, R. J.; Kunz, F. W.; Hoost, T. E. *J. Catal.*, **1997, 166**: 67

14   Wei, Z. L.; Li, H. M.; Zhang, X. Y.; Yan, S. H.; Lv, Z.; Chen, Y. Q.; Gong, M. C. *J. Alloy. Compd.*, **2008, 455**: 322

15   Cai, L.; Zhao, M.; Pi, Z.; Gong, M. C.; Chen, Y. Q. *Chin. J. Catal.*, **2008, 29**: 108 [蔡 黎, 赵 明, 皮 展, 龚茂初, 陈耀强. 催化学报, **2008, 29**: 108]

16   Yao, S. Y.; Xie, Z. H. *J. Mater. Process. Tech.*, **2007, 186**: 54

17   Llusar, M.; Pidol, L.; Roux, C.; Pozzo, J. L.; Sanchez, C. *Chem. Mater.*, **2002, 14**: 5124

18   Du, J. M.; Liu, Z. M.; Li, Z. H.; Han, B. X.; Huang, Y.; Zhang, J. L. *Micropor. Mesopor. Mater.*, **2005, 83**: 145

19   Capel-Sanchez, M. C.; Campos-Martin, J. M.; Fierro, J. L. G. *J. Catal.*, **2005, 234**: 488

20   Sing, K. S. W.; Everett, D. H.; Haul, R. A. W.; Moscou, L.; Pierotti, R. A.; Rouquerol, J.; Siemieniewska, T. *Pure Appl. Chem.*, **1985, 57**: 603

21   Sugiura, M.; Ozawa, M.; Suda, A.; Suzuki, T.; Kanazawa, T. *Bell. Chem. Soc. Jpn.*, **2005, 78**: 752

22   Kaspar, J.; Fornasiero, P.; Hickey, N. *Catal. Today*, **2003, 77**: 419

23   Dimonte, R.; Kaspar, J.; Fornasiero, P.; Graziani, M.; Pazé, C.; Gubitosa, G. *Inorg. Chim. Acta*, **2002, 334**: 318

24   Prinatto, F.; Ghiotti, G.; Nova, I. *J. Phys. Chem. B*, **2001, 105**: 12732